Preprints.org

Article

Not peer-reviewed version

Evaluation of Geographical and Annual Changes in Rice Planting Patterns with Satellite Images in Flood-Prone Area of Pampanga River Basin, the Philippines

Kohei Hosonuma , Kentaro AIDA , Vicente Jr Ballaran , Naoko Nagumo , Patricia Ann J Sanchez , Tsuyoshi SUMITA , Koki Homma *

Posted Date: 31 October 2023

doi: 10.20944/preprints202310.2027.v1

Keywords: Philippines; flood-prone area; MODIS; time-series data; remote sensing; rice

Preprints.org is a free multidiscipline platform providing preprint service that is dedicated to making early versions of research outputs permanently available and citable. Preprints posted at Preprints.org appear in Web of Science, Crossref, Google Scholar, Scilit, Europe PMC.

Copyright: This is an open access article distributed under the Creative Commons Attribution License which permits unrestricted use, distribution, and reproduction in any medium, provided the original work is properly cited.

Preprints (www.preprints.org) | NOT PEER-REVIEWED | Posted: 31 October 2023 doi:10.20944/preprints202310.2027.v1

Disclaimer/Publisher's Note: The statements, opinions, and data contained in all publications are solely those of the individual author(s) and contributor(s) and not of MDPI and/or the editor(s). MDPI and/or the editor(s) disclaim responsibility for any injury to people or property resulting from any ideas, methods, instructions, or products referred to in the content.

Article

Evaluation of Geographical and Annual Changes in rice Planting Patterns with Satellite Images in Flood-prone area of Pampanga River Basin, the Philippines

Kohei Hosonuma [1], Kentaro Aida [2], Vicente Jr Ballaran [2,3], Naoko Nagumo [2], Patricia Ann Sanchez [3], Tsuyoshi Sumita [1] and Koki Homma [1,*]

[1] Graduate School of Agricultural Science, Tohoku University, Sendai 9808572, Japan
[2] The International Center for Water Hazard and Risk Management, Tsukuba 3058516, Japan
[3] The University of the Philippine Los Baños, Los Baños 4031, Philippine
* Correspondence: koki.homma.d6@tohoku.ac.jp

Abstract: Floods are some of the most devastating crop disasters in Southeast Asia. The Pampanga River Basin in the Philippines is a representative flood-prone area, where cultivation patterns are varied according to the flood risk. However, quantitative analyses on the effects of flooding on cultivation patterns remain quite limited. Accordingly, this study analyzes MODIS LAI data (MCD15A2H) from 2007 to 2022 to evaluate annual and geographical differences in cultivation patterns in the Candaba municipality of the basin. The analysis consists of two stages of hierarchical clustering: a first stage for area classification and a second stage for the classification of annual LAI dynamics. As a result, Candaba is divided into four areas, which are found to be partly consistent with the observed flood risk. Subsequently, the annual LAI dynamics in each area are divided into two or three clusters. The obvious differences among the clusters are caused by flooding in the late rainy season, delaying the start of planting in the dry season. The clusters also indicate that the cultivation patterns slightly changed over the 16 years of the study period. The results of this study suggest that the two-stage clustering approach provides an effective tool for the analysis of MODIS LAI data when considering cultivation patterns characterized by annual and geographical differences.

Keywords: Philippines; flood-prone area; MODIS; time-series data; remote sensing; rice

1. Introduction

Floods are some of the most devastating disasters, causing significant damage to crops around the world. The FAO has announced that damages to crops and livestock caused by flooding amounted to USD 21 billion, comprising 19% of the total loss caused by all disasters from 2008 to 2018 [1]. In order to reduce the associated damages, cultivation patterns are varied depending on the flood risk in the floodplains of Southeast Asia [2, 3]. Information on cultivation patterns is extremely important for the management and evaluation of flood damage [4]. At present, such information is mainly collected through field surveys. However, field surveys mostly fail to provide the geographical distribution of cultivation patterns, as they are conducted on a points basis. Moreover, surveys ordinarily consider a certain management period or growth stage, for example, the planting period or heading stage of cereals. These information constraints limit the ability to evaluate flood damage based on the crop growth stage or inundation depth.

The Pampanga River Basin is located in the central part of Luzon Island in the Philippines, and is one of the largest floodplains and rice-producing areas in Southeast Asia. Floods are frequently caused by monsoons and typhoons during the rainy season, affecting crops in various ways almost every year. For example, during Typhoon "ULYSSES", 4490 hectares of farmland were damaged

© 2023 by the author(s). Distributed under a Creative Commons CC BY license.

Preprints (www.preprints.org) | NOT PEER-REVIEWED | Posted: 31 October 2023 doi:10.20944/preprints202310.2027.v1

throughout the entire province of Pampanga, with agricultural damage amounting to about 200 million pesos [5]. To avoid these damages, farmers have developed various cultivation patterns including fish raising and vegetable cultivation [6]; however, the geographic distribution and annual change of cultivation patterns has not yet been analyzed. Such an analysis would provide important information, helping to evaluate how farmers have adapted to flooding and to develop countermeasures for the future.

Remote sensing using satellite images has been considered as an alternative evaluation method to field surveys, due to the versatility and wide applicability of the obtained information. Vegetation indices or leaf area index (LAI) obtained from satellite images have been employed for the evaluation of crop growth [7, 8], growth stage [9, 10], and cultivation management [11]. The coarse resolution and cloud disturbances are major constraints for the utilization of satellite images [12]; however, previous studies have suggested that the use of statistical procedures on long-term time-series data allow for the detection of changes in cultivation patterns. Iwahashi et al. (2021) used time-series data from the MODIS LAI product and revealed conversion from late-matured to early-matured cultivars and extension of dry season rice cropping in Cambodia [13]. Zhao et al. (2022) used long-term time-series data from the MODIS EVI product and revealed the effect of global warming on the phenological changes of wheat in China [14]. Based on the above information, we evaluated annual and geographical differences in cultivation patterns in the Pampanga River Basin, the Philippines by analyzing long-term time-series MODIS data.

2. Materials and Methods

2.1. Study area

The study was conducted in Candaba municipality, located in the floodplain of the Pampanga River Basin (Figure 1). The area is characterized by a tropical monsoon climate. The rainy season is generally from June to October, during which typhoons of various sizes hit the area. In the rainy season, the several rivers flowing into the area often lead to floods, especially in typhoon events. The floods transform some areas, through inundation, into a complex comprising variably saturated wetland, shallow swamps, and deeper freshwater ponds [15].

Candaba belongs to Region Ⅲ (Central Luzon), and is one of the largest rice-producing area in the Philippines [16]. Rice is the dominant crop in Candaba, but other modes of cultivation, including fish and vegetable cultivation, have also been reported [6]. The cultivation period and times for rice vary, depending on flood and dry cultivation.

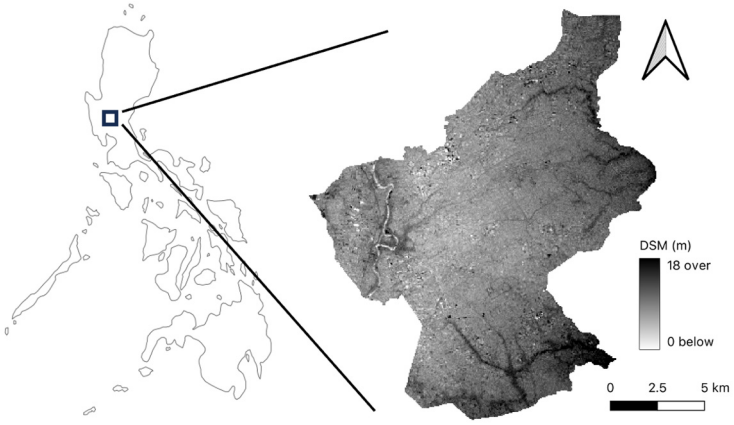

Figure 1. The location of Candaba Municipality. The right figure shows a digital surface model (DSM) of Candaba (ALOS DSM: Global 30m v3.2).

2.2. LAI data

MODIS data (MCD15A2H) were downloaded for the 16 years from 2007 to 2022. MCD15A2H provides Leaf Area Index (LAI) values with 500 m pixel size every 8 days. In this study, the 2013

Preprints (www.preprints.org) | NOT PEER-REVIEWED | Posted: 31 October 2023 doi:10.20944/preprints202310.2027.v1

version of GLCNMO, a raster data set that contains global land-cover information based on MODIS data with 500 m pixel size [17], was used to identify paddy fields. LAI values were extracted from pixels in MCD15A2H which were identified as paddy fields according to GLCNMO.

2.3. Analysis of LAI dynamics

Hierarchical clustering was performed on the extracted LAI data. The cluster analysis was conducted in two stages. In the first stage, hierarchical clustering was performed on the time-series LAI data for 16 years in each pixel (n = 618), in order to classify areas with similar LAI dynamics. In the second stage, hierarchical clustering was performed on the time-series LAI data for one year in each pixel of each area classified in the first stage of hierarchical clustering (n = number of pixels in the area × 15). The one-year data were divided from October of the previous year to September of the target year, in order to include the planting periods of the dry and rainy seasons. Ward's method was employed to calculate the distance between clusters. The thresholds to determine the clusters were set at 60% and 70% of all Euclidean distances in the first and second stages, respectively.

2.4. Software

MCD15A2H was downloaded using Google Earth Engine [18]. LAI data extraction from MCD15A2H was performed using Quantum Geographic Information System (QGIS version 3.14). Hierarchical clustering was performed using the SciPy library in Python (SciPy version 1.7.1).

3. Results

3.1. Area classification in Candaba

First, hierarchical clustering was performed on the MODIS LAI product (MCD15A2H) for the 16 years of the study period (2007–2022). The first stage clearly classified Candaba into four areas: The southern area (Area 1), the northern area (Area 2), the lower terrain area (Area 3), and the eastern and western area (Area 4); see Figure 2.

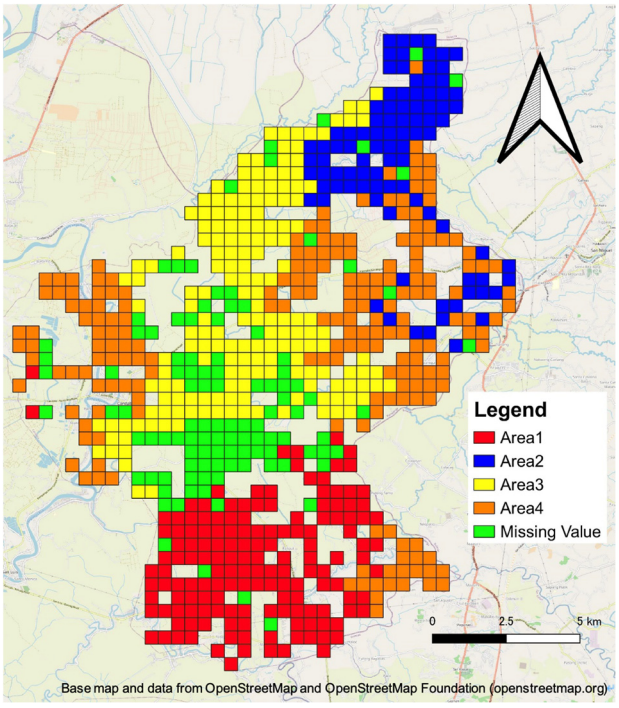

Figure 2. The result of the first stage of hierarchical clustering using MODIS LAI products (2007–2022).

Preprints (www.preprints.org) | NOT PEER-REVIEWED | Posted: 31 October 2023 doi:10.20944/preprints202310.2027.v1

3.2. Annual LAI dynamics for each region

The second stage of hierarchical clustering was performed on the MODIS LAI data to compare the annual LAI dynamics for each area and year.

3.2.1. Area 1 (Southern area)

Area 1 was divided into two clusters. Figure 3 shows the averaged LAI dynamics for each cluster. Both clusters had a large peak during the dry season. Cluster 2 reached its peak earlier than Cluster 1, and the LAI value at the peak was higher than that for Cluster 1. A small peak after the large peak was observed in Cluster 2, and its peak was around the end of the dry season. Figure 4 shows the annual distribution for each cluster. Cluster 1 was frequently observed after 2015, while Cluster 2 was frequently observed before 2014.

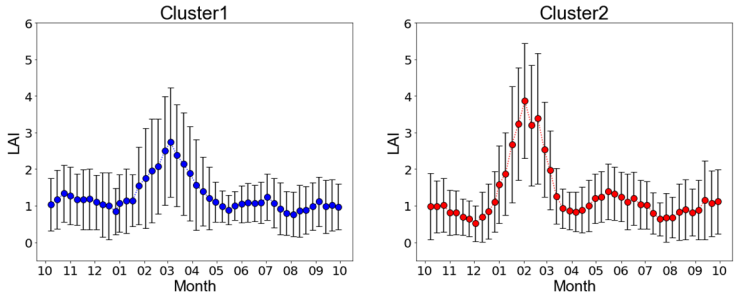

Figure 3. The averaged LAI dynamics for each cluster in Area 1. The clusters were divided in the second stage of hierarchical clustering. Error bars show standard deviations.

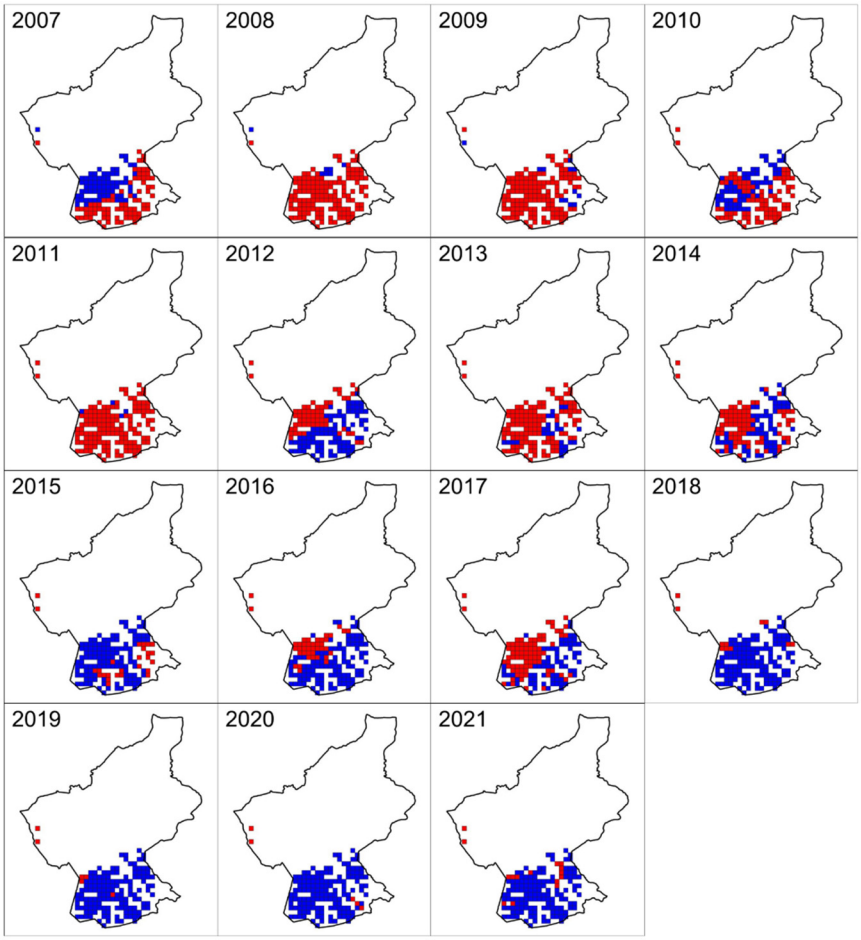

Figure 4. The distribution map for each cluster in Area 1. Blue and red indicate Cluster 1 and Cluster 2 in Figure 3, respectively.

Preprints (www.preprints.org) | NOT PEER-REVIEWED | Posted: 31 October 2023 doi:10.20944/preprints202310.2027.v1

3.2.2. Area 2 (Northern area)

Area 2 was divided into three clusters. Figure 5 shows the averaged LAI dynamics for each cluster. All clusters had three peaks throughout the year. Cluster 2 reached its first peak earlier than the other two clusters. Meanwhile, Cluster 3 reached its first peak later than the other two clusters, but its LAI value was significantly higher than those of the other two clusters. Figure 6 shows the annual distribution for each cluster. The northern part of the area was occupied by Cluster 1 and Cluster 3 from 2007 to 2022, while the southern part of the area transitioned from Cluster 1 to Cluster 2 around 2014.

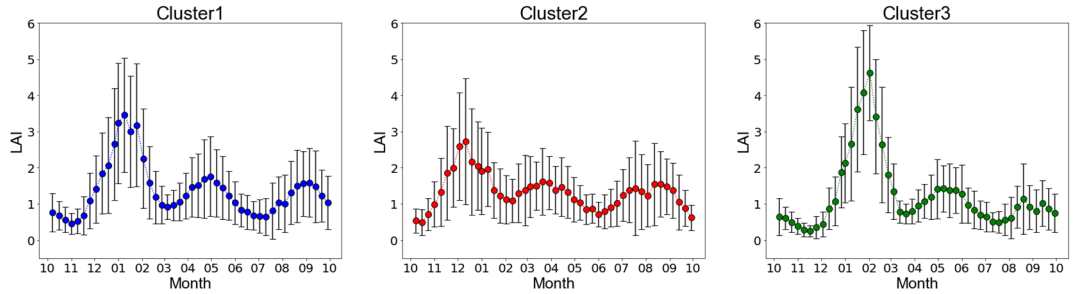

Figure 5. The averaged LAI dynamics for each cluster in Area 2. The clusters were divided in the second stage of hierarchical clustering. Error bars show standard deviations.

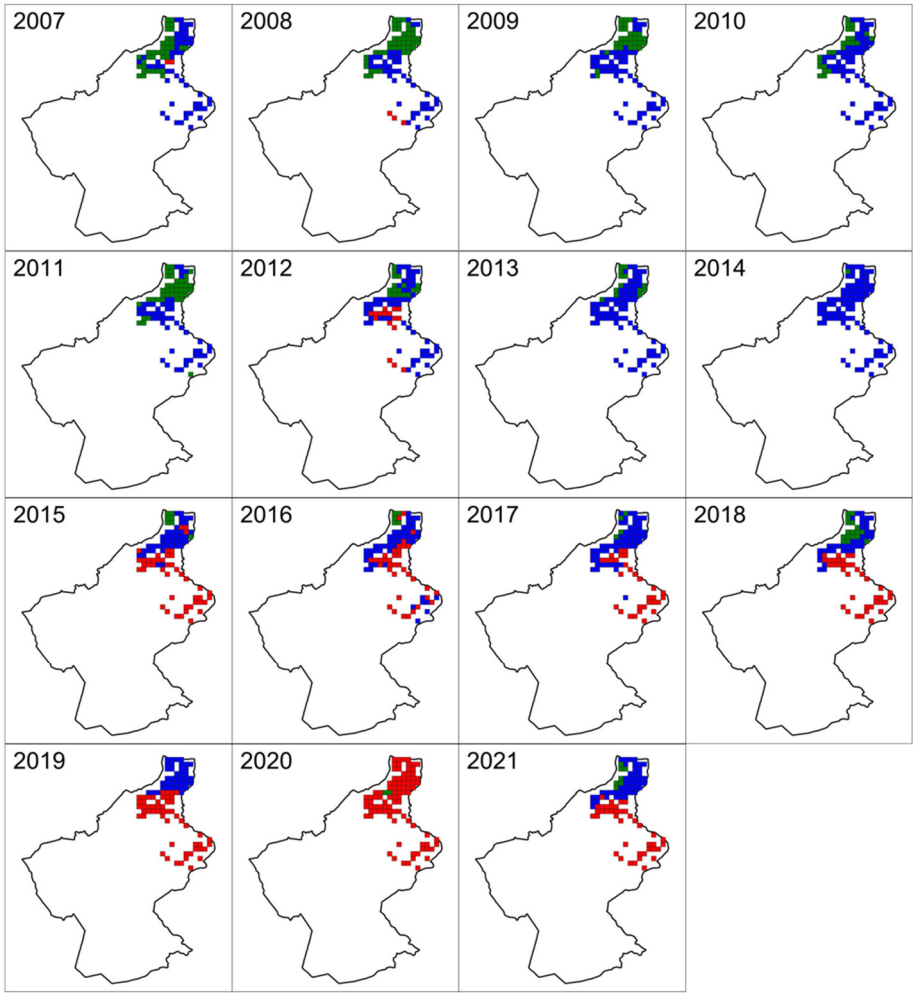

Figure 6. The distribution map for each cluster in Area 2. Blue, red, and green indicate Cluster 1, 2, and 3 in Figure 5, respectively.

Preprints (www.preprints.org) | NOT PEER-REVIEWED | Posted: 31 October 2023 doi:10.20944/preprints202310.2027.v1

3.2.3. Area 3 (Lower terrain area)

Area 3 was divided into three clusters. Figure 7 shows the averaged LAI dynamics for each cluster. All clusters had a large peak during the dry season (first peak) and an additional peak just before the rainy season (second peak). Cluster 3 reached its first peak earlier than the other clusters. Cluster 2 was the latest and had a small peak before its first peak. The LAI value at the second peak of Cluster 3 was higher than that of Cluster 2. Figure 8 shows the annual distribution for each cluster. Cluster 1 occupied the whole area until 2013, while Cluster 3 was more frequently observed after 2014. Cluster 2 occupied the entire area in 2015 and 2020.

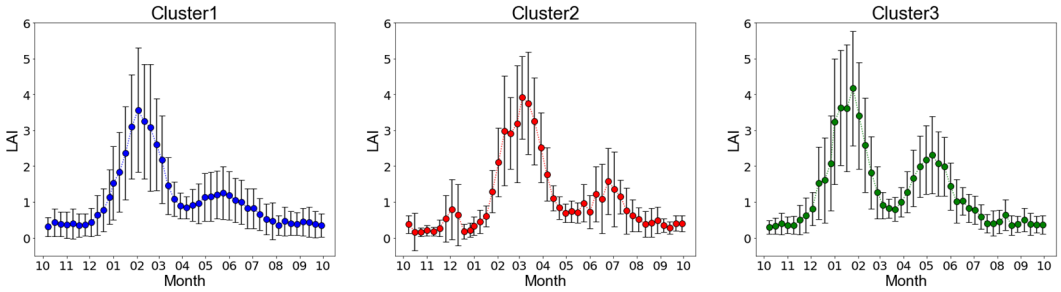

Figure 7. The averaged LAI dynamics for each cluster in Area 3. The clusters were divided in the second stage of hierarchical clustering. Error bars show standard deviations.

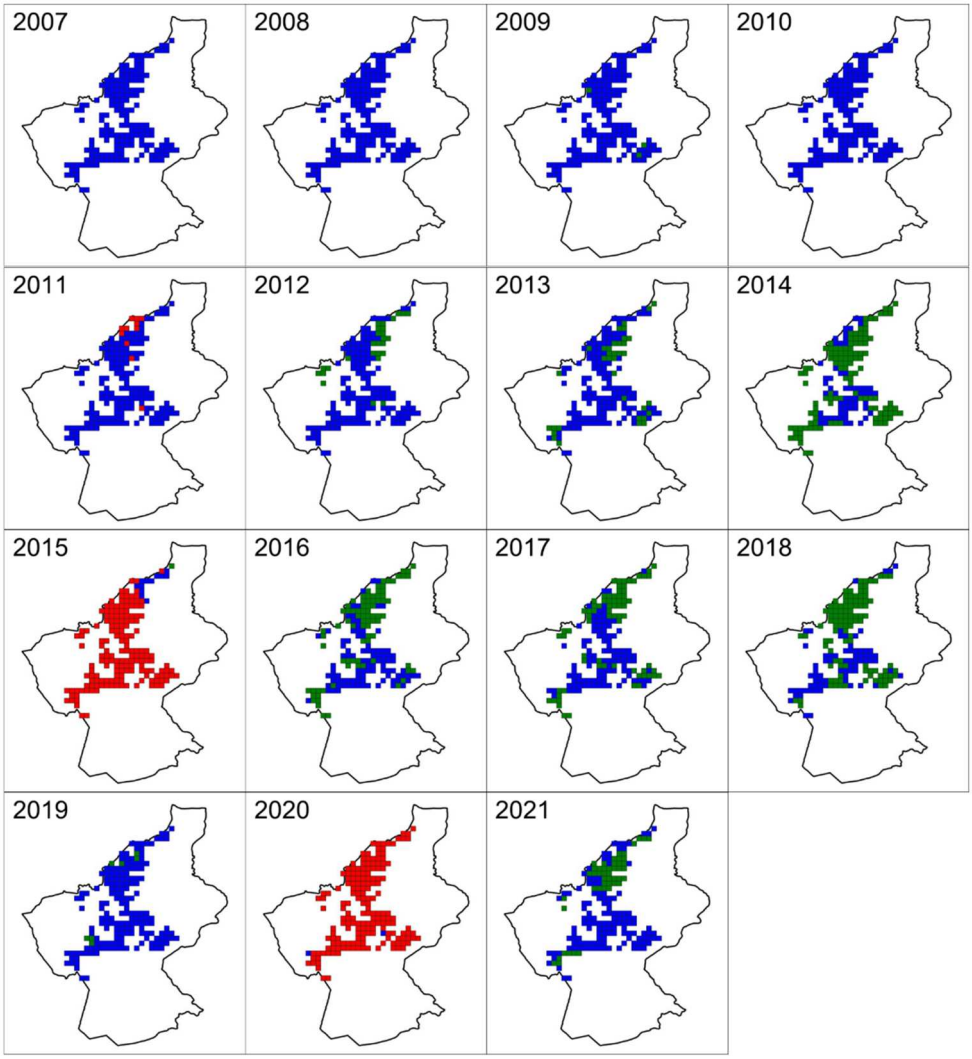

Figure 8. The distribution map for each cluster in Area 3. Blue, red, and green indicate Cluster 1, 2, and 3 in Figure 7, respectively.

Preprints (www.preprints.org) | NOT PEER-REVIEWED | Posted: 31 October 2023 doi:10.20944/preprints202310.2027.v1

3.2.4. Area 4 (Eastern and western area)

Area 4 was divided into three clusters. Figure 9 shows the averaged LAI dynamics for each cluster. The LAI value of Cluster 1 fluctuated between 1 and 2 throughout the year. Cluster 2 had two peaks: August–September and December–January. Cluster 3 had a single peak, in February–March. Figure 10 shows the annual distribution for each cluster. The western area was occupied by Cluster 1 and Cluster 3 from 2007 to 2021. On the other hand, except for the years between 2010 to 2012, most of the eastern area was occupied by Cluster 2.

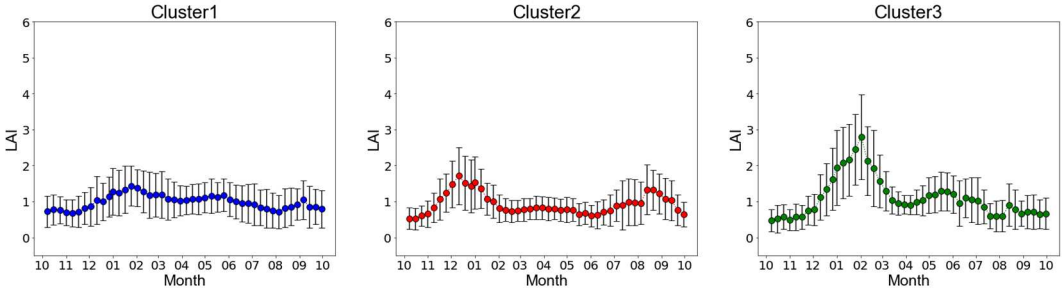

Figure 9. The averaged LAI dynamics for each cluster in Area 4. The clusters were divided in the second stage of hierarchical clustering. Error bars show standard deviations.

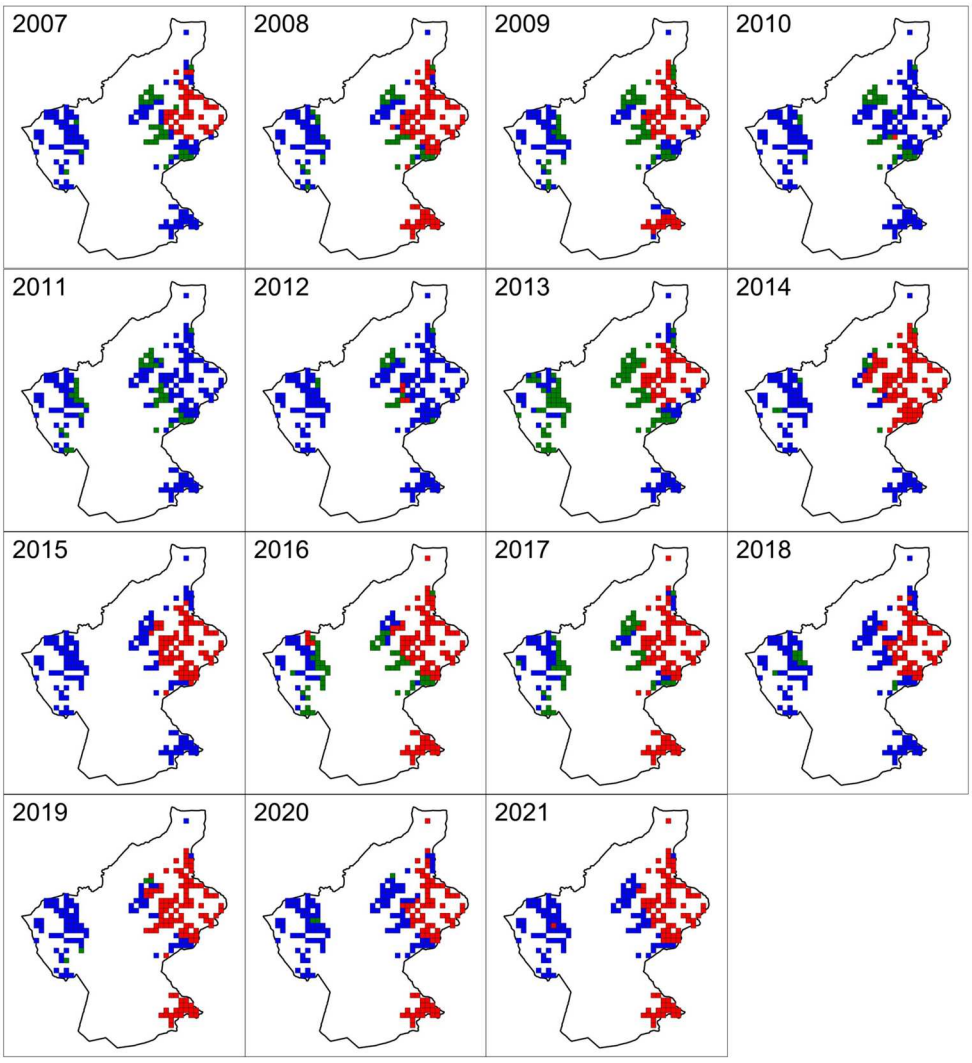

Figure 10. The distribution map for each cluster in Area 4. Blue, red, and green indicate Cluster 1, 2, and 3 in Figure 9, respectively.

Preprints (www.preprints.org) | NOT PEER-REVIEWED | Posted: 31 October 2023 doi:10.20944/preprints202310.2027.v1

4. Discussion

In this study, in order to reveal the differences in the annual LAI dynamics in Candaba, a two-stage clustering analysis was applied: the first stage involved classification of area, while the second stage involved classification of annual LAI dynamics. Direct clustering analysis of annual LAI dynamics without area classification did not yield obvious differences in the LAI dynamics pattern and its geographical distribution (data not shown). As the LAI data for a pixel may include outliers and/or errors, the observation of annual LAI dynamics patterns is often noisy. Increasing the dimensionality by combining 16 years of time-series data allowed for analysis of the geographical differences in LAI dynamics, thus increasing similarity by dividing areas showing similar annual patterns.

In the first stage of classification, Candaba was divided into four areas. As the time-series LAI data were extracted for paddy fields, these areas may reflect local rice cultivation patterns. The classified areas were partly consistent with the geography (Figure 1) and flood areas under the influence of a typhoon (Figure 11). As the timing of cultivation depends on the flood risk in Candaba [6], a map similar to that shown in Figure 2 might be produced by combining the flood risk determined by topography with the experience of farmers. Area 4 presented lower LAI values and obscure peaks, suggesting that rice cultivation was not dominant in this area. This result was expected, as Area 4 occupies relatively higher terrain, where upland crops are sometimes planted (personal communications). Further analysis utilizing finer resolution satellite data may be required for more precise results.

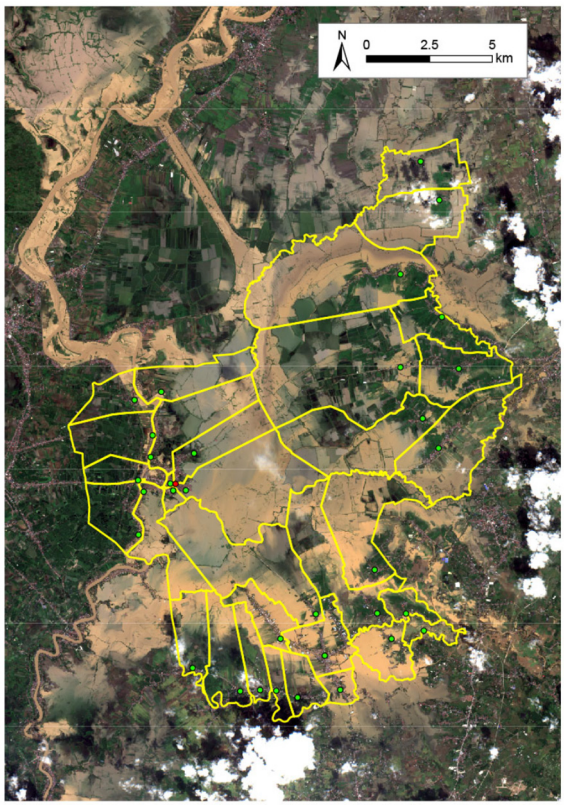

Figure 11. Flood condition after Typhoon Ulysses. The image was obtained from Sentinel-2 on 13 November 2020.

In the second stage of classification, the annual LAI dynamics in each area were divided into two or three clusters. One of the major differences among the clusters was the time of the first (and largest) peak, which seems to reflect the beginning of planting. An earlier first planting generally produced higher second and third peaks. As farmers wait to plant until the flood risk is low, the distribution of clusters might be governed by the flood condition in the rainy season. In particular, Cluster 2 in Area 3, which widely occupied the area in 2015 and 2020, probably indicates that the rice

Preprints (www.preprints.org) | NOT PEER-REVIEWED | Posted: 31 October 2023 doi:10.20944/preprints202310.2027.v1

was damaged and delayed by one month, when compared to the other clusters. Notably, 2015 and 2020 were years that suffered from typhoon damage between November and December. In 2015, typhoon "Nona" passed through the area from December 12th to 17th, and 17 barangays were damaged by flooding [19]. In 2020, typhoon "Ulysses" passed through the area from November 8th to 13th, and 29 barangays were damaged by flooding [5]. According to the agricultural department of the municipal office of Candaba, these typhoons caused a delay in planting during the dry season (personal communications), consistent with the observed LAI dynamics.

Although the largest peak was observed in the dry season, this does not necessarily mean that the area and production of the dry season crop is higher than that in the rainy season. In fact, rainy season crops are also cultivated in areas with low flood risk [6]. The reason why the peak in the dry season appeared to be stronger than that in the rainy season may be that satellite observations are more likely to be disturbed by clouds in the rainy season [20]. Deeply submerged water also disturbs satellite observations [21]. Furthermore, the cultivation in the dry season is more likely to be aligned due to inundation at the end of rainy season, which may be another reason for the enhanced peak observed in the dry season. Melendres (2014) has reported that rice is usually cultivated twice a year in Candaba, but only once in the heart of Candaba Swamp due to flooding in the rainy season [22]. However, the annual LAI dynamics showed 1, 3, and 2 peaks per year in Areas 1, 2, and 3, respectively. This inconsistency might be partly derived from the inadequacy of field surveys, which would not allow for coverage of the whole area.

The annual changes in cluster distribution shown in Figures 4, 6, 8, and 10 suggest that the rice cultivation patterns changed over the 16 years of the study period. For example, Cluster 2 transitioned to Cluster 1 in Area 1, Cluster 1 transitioned to Cluster 2 in the southern part of Area 2, and Cluster 1 partly transitioned to Cluster 3 in Area 3. The transitions in Areas 2 and 3 indicated earlier planting, which would be suitable for double cropping in the dry season. Meanwhile, the transition in Area 1 was accompanied with delayed planting. Although we do not have a reasonable explanation, flood conditions generally lead to delayed planting. Further field surveys would be required for assessment of the flood condition at the beginning of the dry season.

As mentioned above, the long-term time-series MODIS LAI product indicated that cultivation patterns changed over the study period, and are also influenced by floods. However, the cluster analysis appears to have detected little damage to LAI due to flood except for Cluster 2 in Area 3. The low resolution and accuracy of the data may have reduced the detection power for flood damage, and higher resolution satellite data may be required for evaluation of the flood damage [23]. However, low observation opportunity due to cloud cover restricts the application of visible and near-infrared sensors in the rainy season. Synthetic aperture radar (SAR) sensors are often utilized to observe the ground status in rainy season [24, 25]. However, the evaluation of vegetation by SAR generally has low accuracy [26, 27], although that of water bodies due to flooding may be acceptable [28]. Accordingly, combining cultivation patterns (assessed by MODIS) and flood area (by SAR) may provide a promising method for the evaluation of flood damage. In order to develop a real-time monitoring system for flood damage in the context of crop production, detection of the start of cultivation is required. Previous studies have reported that SAR can be used to detect the inundation for preparation of rice cultivation in irrigated paddy fields [29, 30]. However, natural flooding during rice growing or fallowing may disturb such detection in flood-prone environments. The cultivation patterns evaluated in this study may support such cases.

Author Contributions: Conceptualization, K.H.*; data curation, N.N.; formal analysis, K.H.; investigation, K.H., K.A., V.B., P.S., N.N., T.S., and K.H.*; supervision, K.H.*; writing—original draft, K.H.; writing—review and editing, K.H.*

Funding: This work was supported by JST SPRING, Grant Number JPMJSP2114 and by JICA-JST SATREPS, Grant Number JPMJSA 1909.

Data Availability Statement: Publicly available data sets were analyzed in this study. The data can be found here: https://earthengine.google.com/.

Preprints (www.preprints.org) | NOT PEER-REVIEWED | Posted: 31 October 2023 doi:10.20944/preprints202310.2027.v1

Acknowledgments: We are grateful to the students at University of the Philippines Los Baños for helping us conduct the field surveys.

Conflicts of Interest: The authors declare no conflicts of interest.

References

1. The impact of disasters and crises on agriculture and food security: 2021. (2021). In *The impact of disasters and crises on agriculture and food security: 2021*. FAO. https://doi.org/10.4060/cb3673en
2. Marcaida, M., Farhat, Y., Muth, E. N., Cheythyrith, C., Hok, L., Holtgrieve, G., Hossain, F., Neumann, R., & Kim, S. H. (2021). A spatio-temporal analysis of rice production in Tonle Sap floodplains in response to changing hydrology and climate. *Agricultural Water Management*, *258*. https://doi.org/10.1016/j.agwat.2021.107183
3. Molle, F., Chompadist, C., & Bremard, T. (2021). Intensification of rice cultivation in the floodplain of the Chao Phraya delta. *Southeast Asian Studies*, *10*(1), 141–168. https://doi.org/10.20495/seas.10.1_141
4. Win, S., Zin, W. W., Kawasaki, A., & San, Z. M. L. T. (2018). Establishment of flood damage function models: A case study in the Bago River Basin, Myanmar. *International Journal of Disaster Risk Reduction*, *28*, 688–700. https://doi.org/10.1016/j.ijdrr.2018.01.030
5. National Disaster Risk Reduction and Management Center. (2020). *Sitrep No. 28 re Preparedness Measures and Effects for Typhoon "ULYSSES" (I.N. VAMCO)*.
6. Juarez-Lucas, A. M., Kibler, K. M., Ohara, M., & Sayama, T. (2016). Benefits of flood-prone land use and the role of coping capacity, Candaba floodplains, Philippines. *Natural Hazards*, *84*(3), 2243–2264. https://doi.org/10.1007/s11069-016-2551-2
7. Karthikeyan, L., Chawla, I., & Mishra, A. K. (2020). A review of remote sensing applications in agriculture for food security: Crop growth and yield, irrigation, and crop losses. *Journal of Hydrology*, *586*. https://doi.org/10.1016/j.jhydrol.2020.124905
8. Kasampalis, D. A., Alexandridis, T. K., Deva, C., Challinor, A., Moshou, D., & Zalidis, G. (2018). Contribution of remote sensing on crop models: A review. In *Journal of Imaging* (Vol. 4, Issue 4). MDPI. https://doi.org/10.3390/jimaging4040052
9. Araya, S., Ostendorf, B., Lyle, G., & Lewis, M. (2018). CropPhenology: An R package for extracting crop phenology from time series remotely sensed vegetation index imagery. *Ecological Informatics*, *46*, 45–56. https://doi.org/10.1016/j.ecoinf.2018.05.006
10. Hassan, D. F., Abdalkadhum, A. J., Mohammed, R. J., & Shaban, A. (2022). Integration Remote Sensing and Meteorological Data to Monitoring Plant Phenology and Estimation Crop Coefficient and Evapotranspiration. *Journal of Ecological Engineering*, *23*(4), 325–335. https://doi.org/10.12911/22998993/146267
11. Bascietto, M., Santangelo, E., & Beni, C. (2021). Spatial variations of vegetation index from remote sensing linked to soil colloidal status. *Land*, *10*(1), 1–15. https://doi.org/10.3390/land10010080
12. Ozdogan, M., Yang, Y., Allez, G., & Cervantes, C. (2010). Remote sensing of irrigated agriculture: Opportunities and challenges. In *Remote Sensing* (Vol. 2, Issue 9, pp. 2274–2304). https://doi.org/10.3390/rs2092274
13. Iwahashi, Y., Ye, R., Kobayashi, S., Yagura, K., Hor, S., Soben, K., & Homma, K. (2021). Quantification of changes in rice production for 2003–2019 with modis lai data in pursat province, cambodia. *Remote Sensing*, *13*(10). https://doi.org/10.3390/rs13101971
14. Zhao, Y., Wang, X., Guo, Y., Hou, X., & Dong, L. (2022). Winter Wheat Phenology Variation and Its Response to Climate Change in Shandong Province, China. *Remote Sensing*, *14*(18). https://doi.org/10.3390/rs14184482
15. Department of Environment and Natural Resources, Q. C. (2013). *Protected Areas and Wildlife Bureau (2013) The National Wetlands Action Plan for the Philippines 2011–2016*.
16. Mamiit, R. J., Yanagida, J., & Miura, T. (2021). Productivity Hot Spots and Cold Spots: Setting Geographic Priorities for Achieving Food Production Targets. *Frontiers in Sustainable Food Systems*, *5*. https://doi.org/10.3389/fsufs.2021.727484
17. Kobayashi, T., Tateishi, R., Alsaaideh, B., Sharma, R. C., Wakaizumi, T., Miyamoto, D., Bai, X., Long, B. D., Gegentana, G., Maitiniyazi, A., Cahyana, D., Haireti, A., Morifuji, Y., Abake, G., Pratama, R., Zhang, N., Alifu, Z., Shirahata, T., Mi, L., … Phong, D. X. (2017). Production of Global Land Cover Data – GLCNMO2013. *Journal of Geography and Geology*, *9*(3), 1. https://doi.org/10.5539/jgg.v9n3p1

Preprints (www.preprints.org) | NOT PEER-REVIEWED | Posted: 31 October 2023 doi:10.20944/preprints202310.2027.v1

18. Gorelick, N., Hancher, M., Dixon, M., Ilyushchenko, S., Thau, D., & Moore, R. (2017). Google Earth Engine: Planetary-scale geospatial analysis for everyone. *Remote Sensing of Environment*, *202*, 18–27. https://doi.org/10.1016/j.rse.2017.06.031
19. National Disaster Risk Reduction and Management Center. (2015). *Sitrep No. 19 re Preparedness Measures and Effects for Typhoon "NONA" (I.N. MELOR)*.
20. Kim, S.-H., Park, J.-H., Woo, C.-S., & Lee, K.-S. (2005). *Analysis of Temporal Variability of MODIS Leaf Area Index (LAI) Product over Temperate Forest in Korea*.
21. de Grandpré, A., Kinnard, C., & Bertolo, A. (2022). Open-Source Analysis of Submerged Aquatic Vegetation Cover in Complex Waters Using High-Resolution Satellite Remote Sensing: An Adaptable Framework. *Remote Sensing*, *14*(2). https://doi.org/10.3390/rs14020267
22. Melendres, R. G. (2014). *The Utilization of Candaba Swamp from Prehistoric to Present Time: Evidences from Archaeology, History and Ethnography*.
23. Kotera, A., Nagano, T., Hanittinan, P., & Koontanakulvong, S. (2016). Assessing the degree of flood damage to rice crops in the Chao Phraya delta, Thailand, using MODIS satellite imaging. *Paddy and Water Environment*, *14*(1), 271–280. https://doi.org/10.1007/s10333-015-0496-9
24. Ding, X. W., & Li, X. F. (2011). Monitoring of the water-area variations of Lake Dongting in China with ENVISAT ASAR images. *International Journal of Applied Earth Observation and Geoinformation*, *13*(6), 894–901. https://doi.org/10.1016/j.jag.2011.06.009
25. Mendes, F. de S., Baron, D., Gerold, G., Liesenberg, V., & Erasmi, S. (2019). Optical and SAR remote sensing synergism for mapping vegetation types in the endangered Cerrado/Amazon ecotone of Nova Mutum-Mato Grosso. *Remote Sensing*, *11*(10). https://doi.org/10.3390/rs11101161
26. Orynbaikyzy, A., Gessner, U., & Conrad, C. (2019). Crop type classification using a combination of optical and radar remote sensing data: a review. In *International Journal of Remote Sensing* (Vol. 40, Issue 17, pp. 6553–6595). Taylor and Francis Ltd. https://doi.org/10.1080/01431161.2019.1569791
27. Hirooka, Y., Homma, K., Maki, M., & Sekiguchi, K. (2015). Applicability of synthetic aperture radar (SAR) to evaluate leaf area index (LAI) and its growth rate of rice in farmers' fields in Lao PDR. *Field Crops Research*, *176*, 119–122. https://doi.org/10.1016/j.fcr.2015.02.022
28. Grimaldi, S., Xu, J., Li, Y., Pauwels, V. R. N., & Walker, J. P. (2020). Flood mapping under vegetation using single SAR acquisitions. *Remote Sensing of Environment*, *237*. https://doi.org/10.1016/j.rse.2019.111582
29. Jeong, S., Kang, S., Jang, K., Lee, H., Hong, S., & Ko, D. (2012). Development of Variable Threshold Models for detection of irrigated paddy rice fields and irrigation timing in heterogeneous land cover. *Agricultural Water Management*, *115*, 83–91. https://doi.org/10.1016/j.agwat.2012.08.012
30. Supriatna, Rokhmatuloh, Wibowo, A., Shidiq, I. P. A., Pratama, G. P., & Gandharum, L. (2019). Spatio-temporal analysis of rice field phenology using Sentinel-1 image in Karawang Regency West Java, Indonesia. *International Journal of GEOMATE*, *17*(62), 101–106. https://doi.org/10.21660/2019.62.8782

Disclaimer/Publisher's Note: The statements, opinions and data contained in all publications are solely those of the individual author(s) and contributor(s) and not of MDPI and/or the editor(s). MDPI and/or the editor(s) disclaim responsibility for any injury to people or property resulting from any ideas, methods, instructions or products referred to in the content.